VERSITA

GEOCHRONOMETRIA 30 (2008), pp xx-xx
DOI 10.2478/v10003-008-0009-6

Available online at
versita.metapress.com and www.geochronometria.pl

SIMULATION OF OSL PULSE-ANNEALING AT DIFFERENT HEATING RATES: CONCLUSIONS CONCERNING THE EVALUATED TRAPPING PARAMETERS AND LIFETIMES

VASILIS PAGONIS[1] and REUVEN CHEN[2]
[1]*Physics Department, McDaniel College, Westminster, MD21157, USA*
[2]*School of Physics and Astronomy, Raymond and Beverly Sackler Faculty of Exact Sciences, Tel-Aviv University, Tel-Aviv 69978, Israel*

Received 31 January 2007 Accepted 10 March 2008

Abstract: Pulse annealing has been the subject of several studies in recent years. In its basic form, it consists of relatively short-time optically stimulated luminescence (OSL) measurements of a given sample after annealing at successively higher temperatures in, say, 10°C increments. The result is a decreasing function with a maximum OSL at low temperatures and gradually decreasing to zero at high temperature. Another presentation is that of the percentage OSL signal lost per annealing phase, associated with minus the derivative of the former curve, which yields a thermoluminescence (TL)-like peak. When the heating is performed at different heating rates, the TL various heating rates (VHR) method can be utilized to evaluate the trapping parameters. Further research yielded more complex pulse-annealing results in quartz, explained to be associated with the hole reservoir. In the present work, we simulate numerically the effect, following the experimental steps, in the simpler form when no reservoir is involved, and in the more complex case where the reservoir plays an important role. The shapes of the reduction-rate curves resemble the experimental ones. The activation energies found by the VHR method are very close to the inserted ones when the retrapping probability is small, and deviate from them when retrapping is strong. The theoretical reasons for this deviation are discussed.

Keywords: OSL, pulse annealing, lifetime, activation energy.

1. INTRODUCTION

An important issue concerning thermoluminescence (TL) and optically stimulated luminescence (OSL) dating is the stability of the age-dependent signal. In particular, the evaluation of the activation energies and effective frequency factors of the relevant trapping states are of great significance. The method of pulse annealing has been developed for the evaluation of these magnitudes from OSL measurements. This consists of obtaining and displaying the thermal stability by plotting the OSL signal measured at room temperature (RT) or somewhat elevated temperature (say, 50°C) remaining after holding the sample for fixed time at various temperatures (Bøtter-Jensen *et al.*, 2003). Rhodes (1988) used 5 minute heat treatments at a range of temperatures up to 240°C on naturally irradiated sedimentary quartz for the removal of the OSL component which has a low thermal stability. Duller and Wintle (1991) studied TL and infra-red stimulated luminescence (IRSL) in potassium feldspar separates. They describe an experiment of heating the sample to 450°C and monitoring the IRSL signal every 10°C to see how the temperature of the sample affects the magnitude of the IRSL signal.

Bailiff and Poolton (1991) describe "pulse annealing" measurements in feldspars. In their measurement, performed shortly after irradiation, samples were subject to cycles of rapid heating to the selected temperature, cooled to RT and measurement of IRSL using a short duration stimulation was carried out, causing negligible depletion. Duller and Bøtter-Jensen (1993) report on the results of measurements of OSL stimulated by green and infrared light in potassium feldspars. The samples were heated at

Corresponding author: R. Chen
e-mail: chenr@tau.ac.il

ISSN 1897-1695 (online), 1733-8387 (print)

10°C/s and the luminescence signal was measured for 0.1 s every 10°C, both with and without optical stimulation, where the TL signal was measured for comparison. The OSL signal at any temperature was evaluated as the difference between total luminescence and TL. Duller (1994) established the method of pulse annealing for the analysis of high precision data obtained using IRSL measurements. For potassium feldspars, he measured the percentage IRSL signal remaining after annealing to successively increasing temperatures. For different circumstances (natural sample, natural + laboratory irradiation, natural + pre-heating) he plotted the IRSL as a function of temperature. The reported curves have maximum (100%) IRSL up to ~250°C, which then gradually decreases to practically zero at ~400°C. The short IR light pulse only monitors the relevant concentration of trapped carriers without bleaching the sample appreciably. Thus, the recorded IRSL is a measure to the concentration of trapped carriers at different temperatures. Duller (1994) also described the same results, plotting the percentage IRSL signal lost per annealing phase of 10°C. The results have a peak shape which resembles a TL peak. This is not too surprising because the procedure depicts in effect an approximation to the negative derivative of the relevant concentration which, under certain conditions, should resemble a simple TL peak (see below).

Short and Tso (1994) described a way of evaluating the activation energies from the descending OSL intensity vs. temperature curves. Their OSL curves vs. temperature are computer generated using the general-one-trap (GOT) approximation, and their retrieved activation energies are in good agreement with the parameters taken in the simulation. Huntley *et al.* (1996) describe "thermal depopulation" in quartz, and from curve fitting of the descending OSL signal following subsequent heating to different temperatures up to 400°C, an activation energy of 1.03 eV and a frequency factor of 1.31×10^{8} s^{-1} were obtained. Li *et al.* (1997) pursued the close analogy between the reduction rate in the OSL intensity of the pulse annealing steps and a TL peak. They performed pulse annealing measurements at different heating rates and assuming relatively simple kinetics, used the various heating rates method for evaluating the relevant activation energy from the shift of the reduction rate curve. For K-feldspar they found an activation energy of 1.72 eV, a frequency factor of 6.1×10^{13} s^{-1} and hence, a lifetime of 10^{9} years at an ambient temperature of 10°C.

Bøtter-Jensen *et al.* (2003) point out that the interpretation of the plots of remaining OSL after a fixed time at various temperatures is complicated by the sensitivity change brought about by thermal treatment. Wintle and Murray (1998) used the response of the 110°C TL peak to a test dose to correct for such sensitivity changes. Li and Chen (2001) studied the pulse annealing results and the derived OSL reduction rate where, like in quartz, holes from a reservoir replenish the hole centre during the heating stage, thus yielding a peak-shaped pulse-annealing curve. The reduction rate curve derived from this has a negative minimum and a positive maximum. Both of them shifted with the heating rate. Assuming first-order behaviour, Li and Chen (2001) evaluated the trapping parameters and from them estimated their lifetimes at 20°C for the OSL trap and the reservoir. A further study of the thermal stability and pulse annealing in quartz was given by Li and Li (2006). Pulse annealing was also mentioned (Bulur *et al.* 2000, Singarayer and Bailey 2003) with regard to the linear modulation technique (LM-OSL).

In the present work, we report on our results of simulation of the pulse-annealing effect within a framework of a model with a trapping state, a recombination centre and a reservoir. We show that, as could be expected, the numerical results are qualitatively rather similar to the experimental results in quartz as given by Li and Chen (2001). The results of the activation energies evaluated from simulation of the various heating rate measurements deviate in some cases from the values inserted into the simulation program; the reasons for this are discussed.

2. THEORETICAL CONSIDERATIONS

The simplest, first-order kinetics of luminescence as given by Randall and Wilkins (1945) assumes that the rate of change of concentration of trapped electrons following appropriate excitation is given by

$$-\frac{dn}{dt} = sn\exp\left(-\frac{E}{kT}\right) \tag{2.1}$$

where n (cm^{-3}) is the concentration of trapped electrons at time t (s) and temperature T (K), where $T(t)$ is the heating function. E (eV) is the activation energy, s (s^{-1}) the frequency factor and k (eV/K) the Boltzmann constant. In the case of thermoluminescence, the solution of this simple differential equation for a linear heating function, $T = T_o+\beta t$, where β (K/s) is the constant heating rate, is

$$n = n_0\exp\left[-\left(\frac{s}{\beta}\right)\int_{T_0}^{T}\exp\left(-\frac{E}{kT'}\right)dT'\right] \tag{2.2}$$

The TL intensity is assumed to be $I = -dn/dt$ which yields, by differentiation of **Eq. 2.2** with respect to temperature,

$$I = -\frac{dn}{dt} = -\beta\frac{dn}{dT} = n_0 s\exp\left(-\frac{E}{kT}\right)\exp\left[-\left(\frac{s}{\beta}\right)\int_{T_o}^{T}\exp\left(-\frac{E}{kT'}\right)dT'\right] \tag{2.3}$$

By equating the derivative of **Eq. 2.3** with respect to the temperature T to zero, one gets the condition for maximum temperature

$$\frac{\beta E}{kT_m^{\,2}} = s\exp\left(-\frac{E}{kT_m}\right) \tag{2.4}$$

As shown by Hoogenstraaten (1958), the peak temperature T_m shifts to higher temperatures with increasing

heating rate β. A plot of $\ln(T_m^2/\beta)$ as a function of $1/T_m$ is expected to yield a straight line. From its slope E/k, the activation energy can be readily evaluated. Chen and Winer (1970) showed that **Eq. 2.4** holds also for non-linear heating rates where β is replaced by β_m, the instantaneous heating rate at the maximum. The equation is also approximately correct for second- and general-order peaks. It has also been shown (see e.g. Chen and McKeever, 1997, p. 121) that even in more complex situations, where the governing equation is

$$-\frac{dn}{dt} = s\exp\left(-\frac{E}{kT}\right)f(n) \tag{2.5}$$

where $f(n)$ is a "well behaved" function of the concentration, the various heating rates method should yield good approximate results. This includes the cases of second and general-order kinetics where $f(n) \propto n^2$ and $f(n) \propto n^b$ ($b \neq 1, 2$), respectively. The most general TL situation, however, cannot be presented as **Eq. 2.5** (see below).

The initial idea about the pulse annealing procedure of OSL was as follows (Duller, 1994; Li *et al.*, 1997). In the simplest case of first-order kinetics, the decline of the concentration of trapped electrons with temperature is given by **Eq. 2.2**. If we use a relatively short light exposure for monitoring the concentration, we expect that the stimulating light will not change appreciably this concentration and that the intensity I of measured OSL will be

$$I = Cn \tag{2.6}$$

where C is a constant. If we repeat this measurement following successive stages of annealing to increasing temperatures at steps of, say, 10°C, cooling in each cycle to room temperature (RT) or somewhat higher temperature (say, 50°C) and illuminate by stimulating light for, say, 0.1 s, we get a decreasing function of the signal vs. T, which actually represents $n(T)$. An example can be seen in **Fig. 1** in Duller (1994). When the kinetics details are more complex (see **Eq. 2.5**), the decreasing function $n(T)$ may be of a somewhat different form. Duller has also presented the same results as percentage OSL (IRSL in his case) lost per annealing cycle. These magnitudes represent an approximation to the derivative of $n(T)$ with respect to temperature, which, at least for constant heating rate, is analogous to the TL intensity. Let us denote by $n(T_1)$ and $n(T_2)$ two concentrations at subsequent temperatures T_1 and T_2 in the pulse annealing sequence. As pointed out, these are monitored by short OSL measurements. Let us define

$$\Delta n = n(T_2) - n(T_1) \tag{2.7}$$

Note that, at least in the cases mentioned so far, Δn is expected to be negative. In fact, one measures $\Delta I_{OSL} = I_{OSL}(T_2) - I_{OSL}(T_1)$, and under these circumstances, one gets

$$\Delta I_{OSL} \propto \Delta n \tag{2.8}$$

One has to remember that within the framework of the model discussed so far, both sides of the **Expression 2.8** are negative. For very small temperature steps ΔT, one obviously has

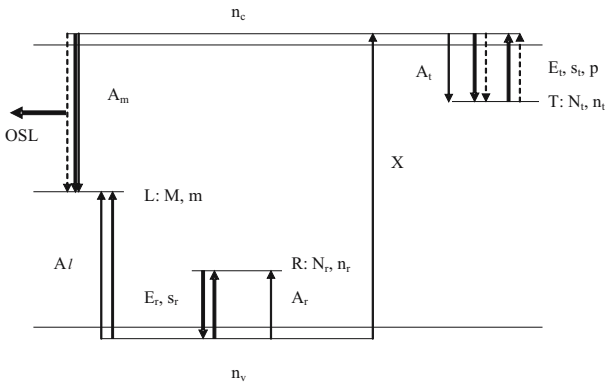

Fig. 1. *Energy level diagram of one electron trapping state, T, one kind of recombination centre, L, and one reservoir, R. Transitions occurring during excitation are given by solid lines, those occurring during the heating are given by thick lines, and transitions taking place during heating, by dashed lines. The meaning of the parameters is given in the text.*

$$\frac{dn}{dT} \cong \frac{\Delta n}{\Delta T} \tag{2.9}$$

whereas for larger values of ΔT, the right hand side is an approximation to the derivative. In the analogous situation of TL, the above discussion mentions that $I = -dn/dt$. Remembering that dn/dT in **Eq. 2.9** is negative, we can see that the analogue to TL intensity in pulse annealing is

$$-\frac{dn}{dt} \cong -\beta\frac{\Delta n}{\Delta T} \tag{2.10}$$

and using **Eq. 2.8**, we can write that

$$-\frac{dn}{dt} \propto -\beta\frac{\Delta I_{OSL}}{\Delta T} \tag{2.11}$$

As long as $\Delta T = T_2 - T_1$ is constant, as indeed is the case in the reported measurements, we can write

$$-\frac{dn}{dt} \propto -\beta \cdot \Delta I_{OSL} \tag{2.12}$$

In view of the remark made above, both sides of **Expression 2.12** are positive; comparison with **Eq. 2.3** above makes the analogy with TL closer. Like in **Eq. 2.3**, the factor β in front of dn/dT does not change the temperature of the maximum; it is the variation of β appearing within the square brackets on the right-hand side expression that causes the shift of the maximum temperature. This is, in essence what was done by Duller (1994) and by Li *et al.* (1997). Once the analogy between TL and pulse-annealed OSL has been established, the way to use the various heating rates methods explained above was open.

Li and Chen (2001) made an important step forward. As pointed out above, they reported on a peak-shaped curve of the pulse-annealed OSL in quartz. As is known (Zimmerman, 1971), TL results in quartz are associated with the existence of a hole reservoir from which holes

may be thermally transferred into the recombination centre, thus contributing to an increase of the sensitivity. **Equation 2.6** above, which meant that I∝n in the simplest situation, may have a different meaning here because the magnitude C is increasing in a certain range during the heating due to the transfer of holes from the reservoir. In the measurements of pulse-annealed OSL, the result is a peak-shaped curve as a function of temperature. The intuitive explanation is that C in **Eq. 2.6** increases due to the transfer of holes from the reservoir, which increases the measured pulse-annealed OSL in the relevant temperature range; this reaches a maximum and starts to decrease at higher temperature where either trap population or the recombination-centre population is depleted and the curve goes down to zero. When the OSL reduction rate in quartz is plotted as a function of temperature, a negative minimum is seen at ~280°C and a positive maximum at ~330°C (see Fig. 2 by Li and Chen, 2001). These are associated with the inflection points in the original plot of the OSL signal vs. the annealing temperature. Li and Chen (2001) assumed that both the transfer of holes from the reservoir and the recombination process are approximately of first order, and used the shift of these (negative and positive) peaks with the heating rate to evaluate the relevant parameters, activation energies and frequency factors.

In the next section, we describe the simulation of pulse-annealed OSL, following step by step the experimental procedure, and using a model with one trapping state, one kind of recombination centre and one hole reservoir. Obviously, the number of trapping states and centres in quartz is significantly larger (Bailey, 2001), but the model used permits us to explain the essence of the effects associated with pulse annealing. We demonstrate the occurrence of the peaks in pulse annealing and monitor the variation of the maximum and minimum temperatures with heating rates. We then draw conclusions concerning the circumstances under which one can expect to get accurately the associated trapping parameters.

3. MODEL AND SIMULATIONS

Figure 1 shows the energy level diagram used for simulating the pulse-annealing OSL. This, in fact, is identical to the Zimmerman (1971) model explaining the predose sensitization effect in quartz in its simplest form, namely, when only one reservoir is involved. Here, T is the electron trapping state with total concentration of N_t (cm^{-3}) and instantaneous occupancy of n_t (cm^{-3}), activation energy of E_t (eV) and frequency factor s_t (s^{-1}), and retrapping probability coefficient of A_t (cm^3s^{-1}). L is the hole recombination centre with total concentration of M (cm^{-3}), instantaneous occupancy m (cm^{-3}), a probability coefficient A_l (cm^3s^{-1}) of trapping holes from the valence band and a recombination probability coefficient A_m (cm^3s^{-1}). R is the hole reservoir with total concentration of N_r (cm^{-3}) and instantaneous occupancy n_r (cm^{-3}). The activation energy for freeing holes is E_r (eV), the corresponding frequency factor is s_r (s^{-1}) and the retrapping probability for holes is A_r (cm^3s^{-1}). n_c (cm^{-3}) and n_v (cm^{-3}) are, respectively, the instantaneous concentrations of free electrons and holes in the conduction and valence bands. X ($cm^{-3}s^{-1}$) is the rate of production of electron-hole pairs, which is proportional to the excitation dose rate. Thus, if the length of excitation is t_D (s), the total concentration of produced electron-hole pairs is $X \cdot t_D$ (cm^{-3}), which is proportional to the imparted dose. p (s^{-1}) is a magnitude proportional to the stimulating light intensity in the OSL measurement stage.

The kinetic equations governing the process along the different stages are as follows,

$$\frac{dn_t}{dt} = A_t(N_t - n_t)n_c - n_t s_t \exp(-E_t / kT) - pn_t \quad (3.1)$$

$$\frac{dn_r}{dt} = A_r(N_r - n_r)n_v - n_r s_r \exp(-E_r / kT) \quad (3.2)$$

$$\frac{dm}{dt} = A_l(M - m)n_v - A_m m n_c \quad (3.3)$$

$$\frac{dn_c}{dt} = X - A_t(N_t - n_t)n_c - A_m m n_c + pn_t \quad (3.4)$$

$$\frac{dn_v}{dt} = \frac{dn_t}{dt} + \frac{dn_c}{dt} - \frac{dn_r}{dt} - \frac{dm}{dt} \quad (3.5)$$

The stages of the experimental procedure are excitation, relaxation, thermal activation and optical stimulation. During excitation, X has nonzero value, the temperature is kept constant at RT (20°C), and p is set to zero. During the relaxation period, the temperature remains the same, X is set to zero and p is still zero. In the annealing stage, both X and p are kept at zero value, and the temperature is increased linearly, with a heating rate β of between 0.5 and 3 K/s at each stage of the pulse annealing. Finally, for the stimulation stage, we cool the sample to 50°C quickly, set p at a constant value (of, say, p = 0.01 s^{-1}), keep $X = 0$ and monitor the simulated OSL for 0.1 s, assuming that the intensity of the emitted light is given by

$$I(t) = A_m m n_c \quad (3.6)$$

and integrating over the stimulation time of 0.1 s. The contribution of the thermally released electrons and holes is taken into consideration in all the stages, however, with the given values of the parameters these had real influence only at the high temperatures of the annealing stage. This permitted the use of the alternative way of evaluating the integral over $I(t)$ as given in **Eq. 3.6** at the stimulation stage (see e.g. Chen *et al.*, 2006). When the number of thermally stimulated carriers is negligible, as we assume for the phase of optical stimulation, the total OSL collected during a length of time t_f has been shown to be

$$\int_0^{t_f} I(t)dt = m_0 - m_f \quad (3.7)$$

where m_o and m_f are, respectively, the occupancy of the recombination centre at the beginning and the end of the optical stimulation time t_f.

The Mathematica and Matlab ode23 solvers have been used for the numerical solution of the simultaneous differential equations, and the results were in excellent agreement. Also, the two ways of integrating the OSL emitted light, namely, numerical integration over **Eq. 3.6** or the use of **Eq. 3.7** gave the same results.

Figure 2 presents the result of simulations of the pulse-annealed OSL in the simple situation where the reservoir plays no role (Duller, 1994; Li *et al.*, 1997). The parameters chosen for this simulation were E_t = 1.78 eV; $s_t = 1.79\times10^{14}$ s^{-1}; $A_t = 10^{-13}$ cm^{3}s^{-1}; $N_t = 10^{13}$ cm^{-3}; $M = 10^{14}$ cm^{-3}; $A_m = 10^{-12}$ cm^{3}s^{-1}; $A_l = 10^{-12}$ cm^{3}s^{-1}; p = 0.01 s^{-1}. The heating rates used were 0.5, 1, 2 and 3 K/s and the steps of the pulse annealing were of ΔT = 5°C (as compared to 10°C in the experiment by Li and Chen). As expected, the OSL curves shifted to higher temperatures with higher heating rates (**Fig. 2a**). In **Fig. 2b**, the OSL reduction rate is shown, yielding TL-like peak-shaped curves which shifted to higher temperatures with increasing heating rates. The inset depicts the plot of $\ln(T_m^2/\beta)$ as a function of $1/(kT_m)$ where T_m is the maximum temperature in **Fig. 2b**. The results yield nearly a straight line, with a slope of E = 1.86±0.05 eV as compared to E_t = 1.78 eV. It should be noted that with ΔT = 10°C, the activation energy was slightly worse, so it seems that due to resolution problems, the smaller is ΔT, the better are the expected results.

Figure 3 shows the results when the reservoir plays an important role, as described by Li and Chen (2001). The additional parameters' values are $N_r = 5\times10^{12}$ cm^{-3}, $A_r = 10^{-10}$ cm^{3}s^{-1}, E_r = 1.33 eV and $s_r = 4.25\times10^{11}$ s^{-1}. The OSL results at the same set of heating rates are shown in **Fig. 3a**. The OSL reduction rate is shown in curve b, as found with ΔT = 5°C. Both the minimum at ~250°C and the maximum at ~290°C shift to higher temperatures with higher heating rates, similarly to the reported experimental results. $\ln(T_n^2/\beta)$ plotted against $1/(kT_n)$ where T_n is the minimum temperature, is shown by triangles on the right hand side of the inset for the minimum, and the fitted straight line yields a slope of 1.26±0.09 eV as compared to the value of E_r = 1.33 eV entered into the simulation. Similar results for the maximum T_m are given by full circles in the inset, and the resulting straight line yields here E = 1.83±0.05 eV as compared to E_t = 1.78 eV. Taking into consideration the finite values of ΔT, these results seem to support the assertion made by Li and Chen (2001) that both the minimum and the maximum result from first-order kinetic processes, and therefore, the various heating rates method is expected to yield the correct activation energies, and hence, the correct lifetime. It should be noted, however, that the low value of the retrapping coefficient chosen (10^{-13} cm^{3}s^{-1}) implies that the processes involved are indeed very close to first order.

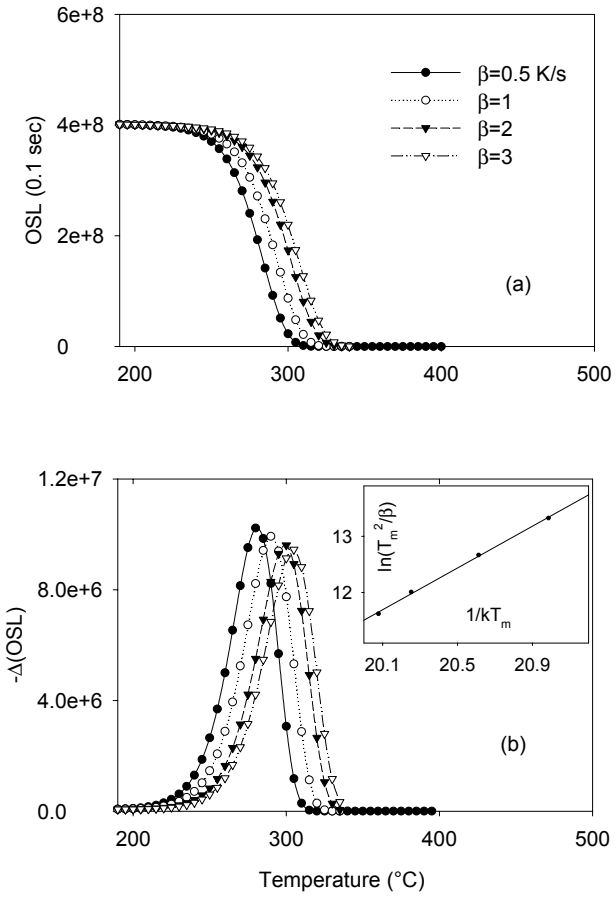

Fig. 2. *Pulse-annealed signal (a) and OSL reduction rate (b) as simulated using a model with one trapping state and one kind of recombination centre with heating rates between 0.5 and 3 K/s. The parameters used for simulation are given in the text. The inset shows $\ln(T_m^2/\beta)$ vs. $1/(kT_m)$, the slope of which yields E_{eff}.*

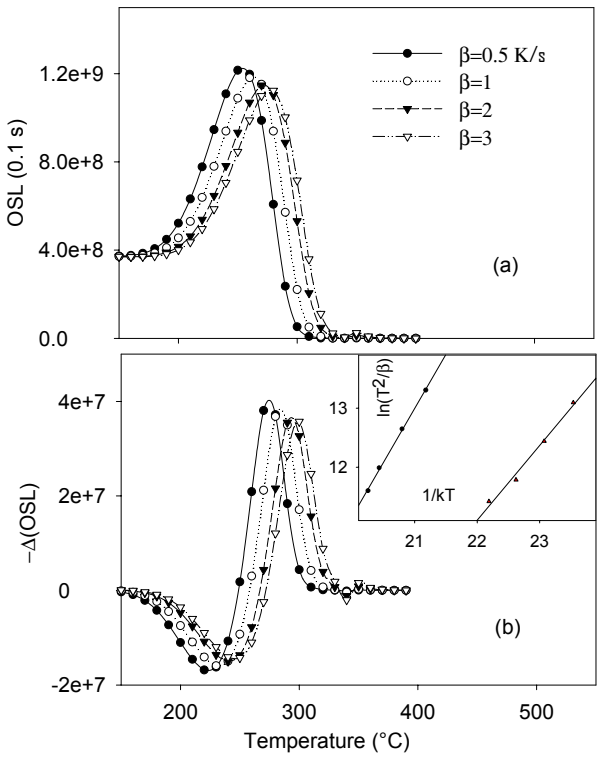

Fig. 3. *Pulse-annealed signal (a) and OSL reduction rate (b) as simulated using a model with one trapping state, one kind of recombination centre and one reservoir, for the same heating rates as in Fig. 2. The parameters are given in the text. The left hand side of the inset shows $\ln(T_m^2/\beta)$ vs. $1/(kT_m)$ for the negative (minimum) peak (•) and the right hand side (Δ) is the same for the positive maximum.*

In order to check the possible implication of non-first-order situations, the run has been repeated with the same set of parameters, except that the retrapping probability has been 3 orders of magnitude larger, namely, $A_t = 10^{-10}$ cm^{3}s^{-1}. The OSL signal results are seen in **Fig. 4a**, and the reduction rates in **4b**. The plot of $\ln(T_m^2/\beta)$ vs. $1/(kT_m)$ is seen in the inset, the full circles for the minimum and the empty circles for the maximum. Note that in the case of the minimum, T_m is, in fact, T_n as mentioned above. The activation energies found from the fitted straight lines were 1.42±0.04 eV for the minimum, as compared to the inserted value of 1.33 eV for the reservoir, and 1.48±0.11 eV for the maximum as compared to 1.78 eV chosen for the trap (see the inset). The deviation from the value used for the simulation as well as the consequences concerning the expected lifetimes at room temperature will be discussed below.

Another point to be mentioned is that in **Fig. 3a**, the curves are practically horizontal up to ~175°C whereas in **Fig. 4a**, they are slightly decreasing in this range. In comparison, curve 1a (natural aliquots) given by Li and Chen (2001) starts nearly horizontally whereas curve 1b (sample annealed at 500°C and irradiated by 50 Gy β dose) is decreasing between 100 and 150°C. We have tried to identify the main reason for this behaviour, and found that the main parameter involved is p, associated with the intensity of the stimulating light. **Figure 5** shows the curves of pulse-annealing OSL for p = 0.01, 0.05 and 0.1 s^{-1}. Whereas in the case of low light intensity the OSL curve is temperature independent up to ~200°C, it yields a decreasing function for higher light intensity up to ~180°C, similarly to the mentioned experimental results.

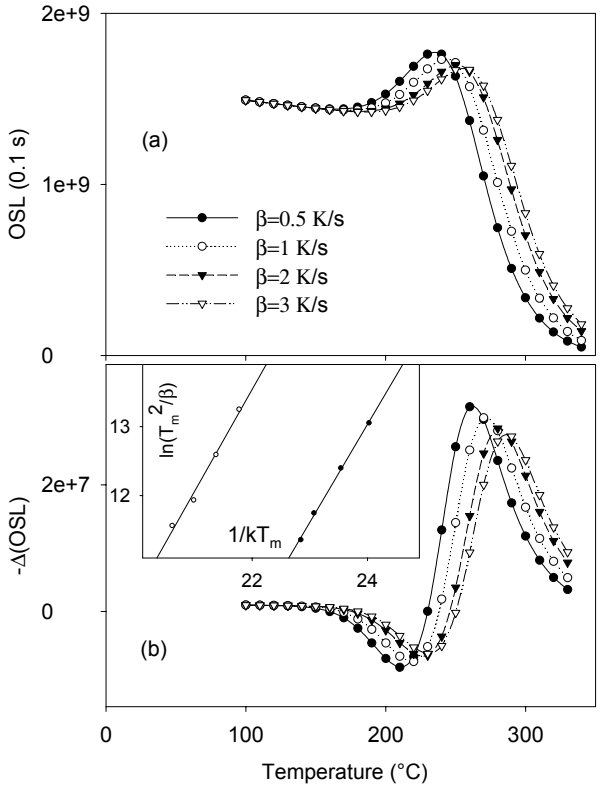

Fig. 4. *Same as Fig. 3, but with significantly larger retrapping probability.*

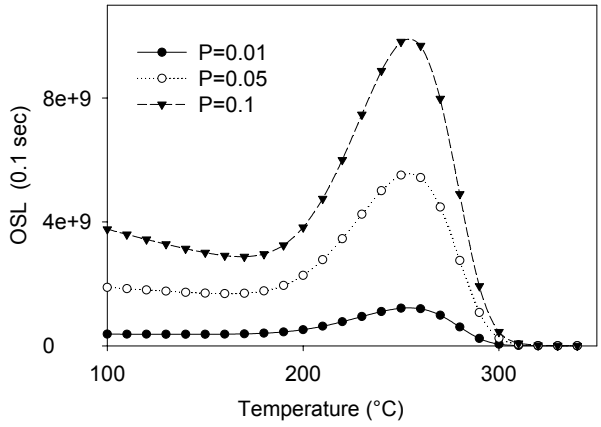

Fig. 5. *Pulse-annealing OSL with low retrapping probability and different values of the stimulating light intensity p, as indicated in the figure.*

4. DISCUSSION AND CONCLUSION

In the present work, we have shown that the pulse-annealing curves previously discussed by Duller (1994) for potassium feldspar and by Li and Chen (2001) for quartz, can be simulated using a relatively simple energy level model. The shape of the remaining percentage IRSL signal as given by Duller and the percentage lost per annealing pulse derived thereof could be simulated using a simple model with one trapping state and one kind of recombination centre. The effect which includes sensitization due to the role of a reservoir, as seen in quartz, could also be simulated. The method of various heating rates (VHR) as used by Li and Chen (2001) has yielded very good results both for the negative minimum and the positive maximum, provided that the retrapping probability was relatively small. With higher values of the retrapping probability, the resulting activation energies were off by up to nearly 20%. This has probably to do with the fact that the VHR method is strictly accurate only for single first-order peaks. The situation here with the trap and reservoir appears to be significantly different when retrapping is strong. The deviation of the effective lifetimes from the "real" lifetimes is rather significant here. For the reservoir, with the chosen parameters, the lifetime $\tau = s^{-1}\exp(E/kT)$ where T = 293 K (RT), is 1.78×10^{11} s or 5630 years. For the evaluated value of 1.42 eV and T_m = 483 K at the minimum, we get $s_{eff} = \frac{\beta E}{kT_m^{\,2}}\exp(E/kT_m) = 2.3\times10^{13}\,s$ which yields for RT, T = 293 K, $\tau = 1.16\times10^{11}$ s = 3700 years, of the same order of magnitude as the correct value. The deviation is larger for the maximum. For E_t = 1.78 eV and $s_t = 1.79\times10^{14}$ s^{-1}, we get at RT $\tau = 2.32\times10^{16}$ s = 7.35×10^{8} y. However, for the evaluated parameters E_t = 1.48 eV and T_m = 531 K we get $s_{eff} = 3.4\times10^{12}$ s^{-1} which yields $\tau = 8.4\times10^{12}$ s = 2.68×10^{5} y at RT, more than three orders of magnitude too low. The conclusion here is that the activation energies reached by the various

heating rates method and the lifetimes derived from them are valuable only if the first-order condition associated with low retrapping holds true.

In an attempt to understand better the underlying reasons for the peak shape of the pulse-annealed OSL signal, we have monitored the simulated concentrations n_t, n_r and m at the end of the irradiation stage with the mentioned set of parameters and with $A_t = 10^{-13}$ cm^{3}s^{-1}. The results are shown in **Fig. 6a**. $n_t(T)$ and $n_r(T)$ are decreasing functions whereas $m(T)$ is first increasing due to the transfer of holes from the reservoir, and then it decreases. One can associate the OSL intensity with the product of m and n_t. This is not a rigorous statement since the effect of the concentration of trapped electrons $n_t(T)$ on the measured OSL takes place through the dependence of the concentration of free electrons $n_c(T)$ on $n_t(T)$. However, the agreement between the OSL curve and the product $m(T)\cdot n_t(T)$ as shown in **Figure 6b** is excellent. The function $m(T)\cdot n_t(T)$ is the product of a peak-shaped function, $m(T)$, and a decreasing function, $n_t(T)$, and therefore the product is also peak shaped, and shifted to lower temperatures compared to $m(T)$. As pointed out, the OSL peak looks practically the same as the product $m(T)\cdot n_t(T)$.

In conclusion, the pulse-annealing results could be simulated and yielded at least qualitatively agreement with experimental results in potassium feldspars and quartz. The use of the method of various heating rates has also been demonstrated in the case of one trapping state and one recombination centre, as well as cases which also include a reservoir. The activation energies and frequency factors were retrievable using the VHR method provided retrapping was relatively low, and then the evaluated lifetimes at RT are reliable. The resolution depended on the size of the temperature step, and the results were more reliable with $\Delta T = 5$°C than with $\Delta T = 10$°C. The evaluated parameters and lifetimes were much less accurate when the retrapping probability was larger.

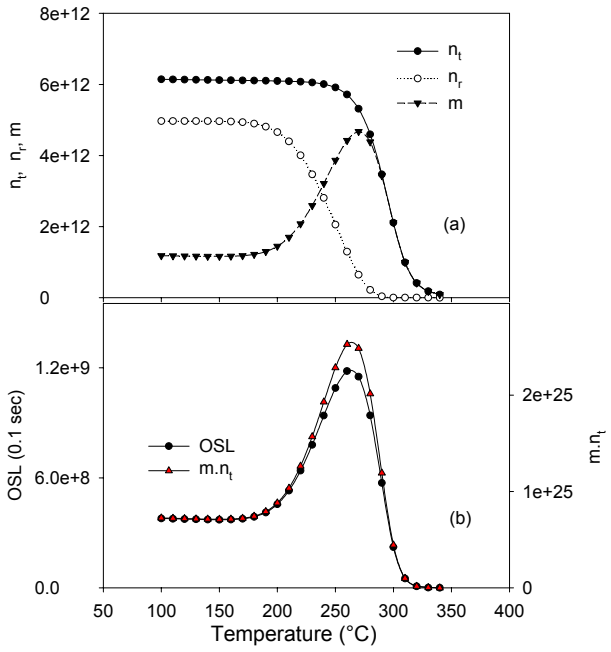

Fig. 6. *For the set of parameters given in the text and with a small retrapping probability $A_t = 10^{-13}$ cm^{3}s^{-1}, the simulated functions $n_t(T)$, $n_r(T)$ and $m(T)$ are shown in (a). The simulated OSL and $m(T)\cdot n_t(T)$ are shown in (b).*

REFERENCES

Bailey RM, 2001. Towards a general kinetic model for optically and thermally stimulated luminescence of quartz. *Radiation Measurements* 33(1): 17-45, DOI 10.1016/S1350-4487(00)00100-1.

Bailiff IK and Poolton RJ, 1991. Studies of charge transfer mechanisms in feldspars. *Nuclear Tracks and Radiation Measurements* 18(1-2): 111-118, DOI 10.1016/1359-0189(91)90101-M.

Bøtter-Jensen L, Ditlefsen C and Mejdahl V, 1991. Combined OSL (infrared) and TL studies of feldspars. *Nuclear Tracks and Radiation Measurements* 18(1-2): 257-263, DOI 10.1016/1359-0189(91)90120-7.

Bøtter-Jensen L, McKeever SWS and Wintle AG, 2003. *Optically stimulated luminescence dosimetry*. Amsterdam, Elsevier: 355 pp.

Bulur E, Bøtter-Jensen L and Murray AS, 2000. Optically stimulated luminescence from quartz measured using the linear modulation technique. *Radiation Measurements* 32(5-6): 407-411, DOI 10.1016/S1350-4487(00)00115-3.

Chen R and Winer SAA, 1970. Effects of various heating rates on glow curves. *Journal of Applied Physics* 41(13): 5227-5232, DOI 10.1063/1.1658652.

Chen R and McKeever SWS, 1997. *Theory of thermoluminescence and related phenomena*. Singapore, World Scientific: 81 pp.

Chen R, Pagonis V and Lawless JL, 2006. The nonmonotonic dose dependence of optically stimulated luminescence in Al_2O_3:C; Analytical and numerical simulation results. *Journal of Applied Physics* 99(3): 0335111-0335116, DOI 10.1063/1.2168266.

Duller GAT, 1994. A new method for the analysis of infrared stimulated luminescence data from potassium feldspars. *Radiation Measurements* 23(2-3): 281-285, DOI 10.1016/1350-4487(94)90053-1.

Duller GAT and Wintle AG, 1991. On infrared luminescence at elevated temperatures. *Nuclear Tracks and Radiation Measurements* 18(4): 379-384, DOI 10.1016/1359-0189(91)90003-Z.

Duller GAT and Bøtter-Jensen L, 1993. Luminescence from potassium feldspars stimulated by infrared and green light. *Radiation Protection Dosimetry* 47: 683-688.

Hoogenstraaten W, 1958. Electron traps in zinc-sulphide phosphors, 1958. *Philips Research Reports* 13: 515-693.

Huntley DJ, Short MA and Dunphy K, 1996. Deep traps in quartz and their use for optical dating. *Canadian Journal of Physics* 74: 81-91.

Li S-H, Tso MYW and Wong NW, 1997. Parameters of OSL traps determined with various heating rates. *Radiation Measurements* 27(1): 43-47, DOI 10.1016/S1350-4487(96)00137-0.

Li S-H and Chen G, 2001. Studies of thermal stability of trapped charges associated with OSL from quartz. *Journal of Physics D: Applied Physics* 34(4): 493-498, DOI 10.1088/0022-3727/34/4/309.

Li B and Li S-H, 2006. Studies of thermal stability of charges associated with thermal transfer of OSL from quartz. *Journal of Physics D: Applied Physics* 39(14): 2941-2949, DOI 10.1088/0022-3727/39/14/011.

Randall JT and Wilkins MHF, 1945. Phosphorescence and electron traps. *Proceedings of the Royal Society of London A* 184: 366-407.

Rhodes EJ, 1988. Methodological considerations in the optical dating of quartz. *Quaternary Science Reviews* 7(3-4): 395-400, DOI 10.1016/0277-3791(88)90035-2.

Short MA and Tso MYW, 1994. New methods for determining the thermal activation energies of light sensitive traps. *Radiation Measurements* 23(2-3): 335-338, DOI 10.1016/1350-4487(94)90061-2.

Singarayer JS and Bailey RM, 2003. Further investigations of the quartz optically stimulated luminescence components using linear modulation. *Radiation Measurements* 37(4-5): 451-458, DOI 10.1016/S1350-4487(03)00062-3.

Wintle AG and Murray AS, 1998. Towards the development of a preheat procedure for OSL dating of quartz. *Radiation Measurements* 29(1): 81-94, DOI 10.1016/S1350-4487(97)00228-X.

Zimmerman J, 1971. The radiation induced increase of the 100°C sensitivity of fired quartz. *Journal of Physics C: Solid State Physics* 4(18): 3265-3276, DOI 10.1088/0022-3719/4/18/032.